Design and Analysis of DC/DC ZCT Boost Converter with Moderate Output Power

Mustafa M. Ibrahim *Khalid M. Abdul-Hassan*
Dep. Of Elec. Engine ering -- College of Engineering
University of Basrah

Abstract:

Soft commutation techniques have been of great interest during the last few years in power supply switching applications. However, freque ncy modulation large conduction losses, and high voltage / current stresses in the switches are known drawbacks

The recently developed Zero-Voltage transition (ZVT) and Zero-Current transition (ZCT) pulse width modulation (PWM) technique incorporated soft-switching function into PWM converters, so that the switching losses can be reduced with minimum voltage / current stresses and circulating energy. The ZCT technique can significantly reduce the switch turn-off loss which is usually the dominant switching loss in high-power applications.

In this papers the steady state analysis and design of the ZCT PWM boost converter are introduced. Control and drive circuit have been designed to drive a 100 Watt ZCT PWM boost converter to experimentally investigate its features and characteristics

تصميم وتحليل مجهز معتدل القدرة Dc/Dc نوع (Boost-ZCT)

الخلاصة:

اكتسبت تقنية التبديل بصورة ناعمة اهتماما متزايدا خلال السنوات الأخيرة في تطبيقات مجهزات القدرة. إلا إن التحكم بالفولتية باستخدام تضمين التردد (frequency modulation) له مفاقيد توصيل عالية عندما يكون المفتاح On واجهادات الفولتية/التيار التي يتعرض لها المفتاح تكون كبيرة.

حديثاً طورت تقنيات الـ (PWM) باستخدام تقنية تحويلة الفولتية صفر (ZVT) وتحويلة التيار صفر (ZCT) حيث تطبيق عملية التبديل بصورة ناعمة في مجهزات القدرة مع تقليل مفاقيد المفتاح واجهادات الفولتية والتيار ودوران الطاقة ضمن مجهز القدرة إلى أدنى حد.

إن تقنية (ZCT) يمكن ان تقلل بشكل فعال مفاقيد التحويل إلى حالة Off في المفتاح التي تمثل المفاقيد الأكبر في المفتاح في تطبيقات القدرات العالية.

وفي هذا البحث نتقدم بتصميم وتحليل الحالة المستقرة لمجهز قدرة نوع (Boost ZCT PWM). لقد صممت دائرة السيطرة للتحكم بمجهز القدرة وبقدرة 100 واط ليبحث خواصه ومميزاته عملياً.

1. Introduction:

Within last few years soft-commutation technique have been of great interest in power-supply switching applications. However, frequency modulation large conduction losses, and high voltage/current stresses in the switches are known drawbacks [2]. In order to overcome these difficulties, many authors have recently proposed alternative topologies One of these topologies that uses an auxiliary switch to provide a dead time to temporarily interrupt the resonance transition has been introduced in [1].

Power semiconductor switches in high-power applications are subjected to high switching stresses and switching losses. To elevate these problems significant derating of device voltage and current ratings and elaborate passive snubbers are usually used, and the switching frequency is limited to low-frequency ranges Generally, a snubber circuit reduces the switching loss and switching stresses of switches, but increases the total power loss in the converter. In recent years, various soft-switching techniques have been proposed to reduce the switching losses and stresses without resorting to bulky and lossy passive snubbers. A good soft-switching scheme for high-power application should reduce the switching losses, diode reverse recovery, and switching stresses for all main and auxiliary switches without increasing the device voltage rating, because the device voltage margin is usually small, and the thermal management is very difficult.

The recently developed zero-voltage transition (ZVT) and zero-current transition (ZCT) pulse width modulation (PWM) techniques incorporate soft-switching function into PWM converters, so that the switching losses can be reduced with minimum voltage and current stresses and circulating energy. The ZVT technique forces the voltage of an incoming switch to zero before its turn-on, to practically eliminate switch turn-on loss. The switch turn-off loss, which is usually the dominating switching loss in high-power application can not be alleviated effectively with the ZVT technique The ZCT technique can significantly reduce the switch turn-off loss by forcing the outgoing switch current to zero prior to its turn-off [3], [4].

Therefore, this paper proposes the ZCT technique using PWM boost DC/DC converter. The converter circuit is shown in Fig. 1 where the shaded area represent the ZCT auxiliary circuit.

2. Operation and Analysis of the ZCT-PWM Boost Converter:

The circuit diagram of the converter is shown in Fig. 1. The operation of this converter is similar to that of its PWM counterpart. The only difference is in the switch turn-on and turn-off transients. During which the auxiliary circuit is actuated to provide soft-switching conditions for the main switch S. Therefore the DC voltage conversion ratio can be calculated as [5]:

$$\frac{V_o}{V_i} = \frac{1}{1-D} \qquad (1)$$

where D is the duty cycle, V_i is the input voltage and V_o is the output voltage.

The waveforms during one switching period are shown in Fig. 2. During one switching period the circuit goes through nine different stages. The

circuits which represent these operating modes are shown in Fig. 3. The operation description starts with switch turn-on transition. Before the main switching turn-on, inductor current "I" is conducted by the main diode, auxiliary current i_x is zero. v_x is a constant positive value. In the whole commutation process the output voltage V_0 and inductor current "I" are assumed to be constant due to the large capacitance and inductance involved. The operating modes of the ZCT-PWM boost converter are:

(a) Turn-on transition I $[T_0,T_2]$ (Fig. 3.a)

At time T_0, S_x is turned on, starting the turn-on transition. The auxiliary resonant tank consisting of L_x and C_x, starts to resonate. The auxiliary current i_x resonates from zero to peak and then decreases towards zero. When i_x reaches zero at T_1, since the resonant capacitor voltage v_x is negative at T_1, the auxiliary circuit continues resonating and i_x reverses its direction and is conducted by D_x, the parallel diode of S_x. Then, S_x can be turned off under zero-current and zero-voltage condition, with much reduced power loss. As i_x increases in positive value, the current of the main diode is diverted into the auxiliary circuit. The equations describing this mode are:

$$v_x(t) = v_x(T_0)\cos(\omega_r(t-T_0)) \qquad (2)$$

$$i_x(t) = -\left[v_x(T_0)\sin(\omega_r(t-T_0))\right]/Z_n \qquad (3)$$

where $\omega_r = 1/\sqrt{L_x C_x}$, $Z_n = \sqrt{L_x/C_x}$

This mode ends at $t=T_2$ when $i_x=I$ and $v_x=0$. The duration of this mode is:

$$\left.\begin{aligned} \tau_1 &= \alpha/\omega_r \\ \alpha &= \sin^{-1}(-IZ_n/v_x(T_0)) \end{aligned}\right\} \qquad (4)$$

where v_{T_0} is the voltage at time T_0

(b) Turn-on transition II $[T_2,T_3]$ (Fig. 3.b)

When i_x reaches its positive peak at T_2, the current in the main diode is reduced to zero. Then, S is turned on under zero-current condition at T_2. The turn-on loss is reduced significantly, since the diode reverse recovery is basically eliminated, and the current rise rate of the switch after turn-on is limited by the resonant inductor. After T_2, i_x decreases rapidly toward zero, since now the output voltage V_0 is included in the resonant path. The state equations describing this mode are:

$$v_x = Z_n I\left[\sin(\omega_1(t-T_2))\right] + V_0\left[\cos(\omega_1(t-T_2))\right] - V_0 \qquad (5)$$

$$i_x = I\left[\cos(\omega_1(t-T_2))\right] - \frac{V_0}{Z_n}\left[\sin(\omega_1(t-T_2))\right] \qquad (6)$$

This mode ends at $t=T_3$ when $i_x=0$ thus the duration of this mode is obtained using eqn (6), so:

$$\left.\begin{aligned} \tau_2 &= \beta/\omega_r \\ \text{where}\quad \beta &= \tan^{-1} Z_n I/V_0 \end{aligned}\right\} \qquad (7)$$

The voltage at the end of this mode can be calculated using eqn.(5)

$$v_x(T_2) = Z_n I\sin\beta + V_0\cos\beta - V_0 \qquad (8)$$

(c) Turn-on transition III $[T_3,T_4]$ (Fig. 3.c)

At T_3, i_x returns to zero, and D_x is turned off naturally. Since the resonant capacitor voltage v_x is positive at T_3, the auxiliary circuit continues resonating, and the negative i_x is conducted by the clamp diode D_c. The state equations describing this mode are:

$$v_x = v_x(T_3)\cos(\omega_r(t-T_3)) \qquad (9)$$

$$i_x = \left[v_x(T_3)/Z_n\right]\sin(\omega_r(t-T_3)) \qquad (10)$$

This mode ends at $t=T_4$ when $i_x=0$, thus from eqn. (10), the duration of this mode is:

$$\tau_3 = \pi / \omega_r \qquad (11)$$

The voltage at the end of this mode can be calculated using eqn.(9)

$$v_x(T_4) = -v_x(T_3) \qquad (12)$$

(d) Switch-on stage $[T_4,T_5]$ (Fig. 3d)

When i_x return to zero again at T_4, D_c is turned off naturally. The auxiliary circuit stops resonating and is disconnected from the main circuit functionally. The converter resumes its PWM operation. The duration of this stage is determined by the PWM control.

(e) Turn-off transition I $[T_5,T_7]$ (Fig.3e)

Before the main switch is turned off, S_x is turned on at T_5. The resonant tank start to resonate again. The resonant path includes L_x, C_x and output voltage v_o. Current i_x is negative, and its magnitude increases from zero to peak and then decreases. When i_x returns to zero at T_6, S_x is turned off under zero-current condition. Since resonant capacitor voltage v_x is less than $-v_o$, the auxiliary circuit continues resonating after T_6, the positive i_x is conducted by D_x, and the current of the main switch is diverted out into the auxiliary circuit. Since D_x clamps the voltage of S_x at particularly zero, the turn-off of S_x is largely eliminated.

The equations describing this mode are:

$$v_x = -V_o[1-\cos(\omega_r(t-T_5))] + v_x(T_5)[\cos(\omega_r(t-T_5))] \qquad (13)$$

$$i_x = -(V_o/Z_n)[\sin(\omega_r(t-T_5))] - v_x(T_5)/Z_n[\sin(\omega_r(t-T_5))] \qquad (14)$$

This mode ends at T_7 when $i_x=I$, thus the duration of this mode can be obtained from eqn (14) as:

$$\tau_4 = \gamma / \omega_r$$

where

$$\gamma = \sin^{-1}(-IZ_n /(V_o - v_x(T_5))) \qquad (15)$$

The voltage at the end of this mode is

$$v_x(T_7) = -V_o[1-\cos\gamma] + v_x(T_5)\cos\gamma \qquad (16)$$

(f) Turn-off transition II $[T_7,T_8]$ (Fig. 3f)

At T_7, i_x reaches I, and the main switch current is reduced to zero, so S is turned off under the zero-current condition. As i_x keeps increasing after T_7, the surplus current will flow through the parallel diode of S and clamp the voltage across S at zero. The gate signal of S can be removed, without causing much turnoff loss.

The equations that describe this mode are the same as those describing mode e of operation.

This operating mode ends at T_8 when $i_x=I$ thus the duration of this mode is.

$$\tau_5 = (3\pi - 2\gamma)/\omega_r \qquad (17)$$

The voltage at the end of this mode can be calculated from eqn.(13) as:

$$v_x(T_8) = -V_o[1-\cos\xi] + v_x(T_5)\cos\xi \qquad (18)$$

where

$$\xi = (3\pi - \gamma)$$

From eqn 17

$$\tau_5 = T_{off} = \sqrt{L_x C_x}(3\pi - 2\gamma)$$

(g) Turnoff transition III $[T_8,T_9]$ (Fig. 3g)

At T_8, i_x falls to I, and the parallel diode of S stops conducting. Since the main diode is still reversely biased, the main inductor current can only flow through the resonant tank, charging the resonance capacitor linearly. The equations that describe this mode are:

$$v_x = 1/C_x(t - T_8) - V_o(1 - \cos\xi) + v_x(T_5)\cos\xi \quad (19)$$

$$i_x = 1 \quad (20)$$

This mode ends at t=T9 when v_x=0, thus, the duration of this mode is:

$$\tau_8 = (C_x V_o / 1)[1 - \cos\xi] - [C_x v_x(T_5)/1]\cos\xi \quad (21)$$

(h) Turnoff transition [T9,T10] (Fig. 3h)

At T_9, v_x is discharged to zero, and the main diode starts to conduct. The resonant tank begin to resonant again. As i_x resonates towards zero, the current in the main diode increase gradually. The state equations that describe this mode are:

$$v_x = Z_n I \sin(\omega_r(t - T_9)) \quad (22)$$

$$i_x = I\cos(\omega_r(t - T_9)) \quad (23)$$

This mode ends at t=T9 when i=0, thus the duration of this mode:

$$\tau_7 = \pi / 2\omega_r \quad (24)$$

The voltage at the end of this mode is

$$v_x = Z_n I \quad (25)$$

(i) Diode on stage [T10,T5] (Fig. 3i)

When i_x returns to zero at T_{10}, the auxiliary circuit stops resonating and is disconnected from the main circuit functionally. The inductor current is conducted by the main diode, and the converter resumes its PWM operation. The duration of this stage is determined by the PWM control.

3. Design of the ZCT auxiliary circuit:

To achieve desirable efficiency improvement by using ZCT technique the auxiliary circuit should be designed to achieved zero-current switching with maximum main current, while keeping the power loss in the auxiliary circuit minimized. The turnoff transition is more critical than the turn-on transition, therefore, the design procedure is mainly based on the turnoff requirement.

3.1 The choice of T_{off}:

To effectively reduce the switch turnoff loss, the duration of turnoff transition 11, $T_{off} = T_8 - T_7$, should be long enough for most storage charge of the main switch to recombine. Using eqn.(17)

$$T_{off} = \sqrt{L_x C_x}(3\pi - 2\sin^{-1}(Z_n I / V_o))$$

$$T_{off} = 2\cos^{-1}(m)\sqrt{L_x C_x}$$

$$T_{off} = T_r \cos^{-1}(m)/\pi \quad (26)$$

where $m = I/I_{pk}$, $T_r = 2\pi\sqrt{L_x C_x}$. I_{pk} is the resonant peak of i_x during turnoff. Assuming v_x is zero at T_5 without losing much accuracy, we can estimate I_{pk} to be

$$I_{pk} = \frac{V_o}{Z_n} \quad (27)$$

Therefore, the choice of T_{off} is device dependent. Generally, T_{off} should be much longer than the current fall time of the switch. A longer T_{off} can be achieved by either increasing I_{pk} of increasing T_r. The design objective is to minimize the conduction loss caused by the soft switching action for a given T_{off}.

3.2 The choice of m (=I/I_{pk})

The design optimization requires power loss models for all switches, diodes and reactive components and is very complex. To simplify the analysis, it is assumed that the power loss caused by the soft switching is proportional to the auxiliary current, i e, the power loss can be represented as a voltage source, the value of which is determine by the components in the resonant path. It is also assumed, without losing much accuracy, that the switch and diodes, S_x, D_y, and D_c

in the auxiliary circuit have the same conduction voltage drop, while the switch and diodes in the main circuit have the same condition voltage drop. Since the auxiliary current is always conducted by L_x, C_x, a switch or a diode in the auxiliary circuit, the voltage drop for the power loss in the auxiliary circuit, denoted as V_c in the following discussion, is constant for all operation stages in the commutation. However, the conduction loss of the main power stage is reduced for $i_x > 0$, but increased for $i_x < 0$. The voltage drop of the main switch (or diode) is assumed to be 1/K of the total voltage in the auxiliary circuit, i.e. V_o/K. Since the charge exchange of the resonant capacitor is equal to the integral of the auxiliary current, the energy loss in the auxiliary circuit per switching cycle can be calculated as

$$E_1 = V_c C_x (4V_o + 4Z_o I) = 2(1+m)V_c I_{pk} T_r / \pi \qquad (28)$$

The current in the main switch or the main diode is $I - i_x$, since i_x changes from negative or positive in the resonance, its net effect on the main circuit conduction loss is nullified for the portion $i_x < I$. So, the additional conduction loss in the main circuit caused by the soft switching is determined only by the portion of i_x where i_x is higher than I in magnitude, as shown in the shaded area in Fig. 2. The resonant energy loss per switching cycle can be calculated as

$$E_2 = 2\left[\left(\sqrt{1-m^2} - m\cos^{-1}(m)\right)/k\right] V_c I_{pk} T_r / \pi \qquad (29)$$

Combining eqn. (28) and eqn. (29), we get the total conduction loss caused by the soft-switching commutation

$$\Delta E = E_1 + E_2 = \left(2V_o I_{pk} T_r / \pi\right)\left[(1+m) + \left(\sqrt{1-m^2} - m\cos^{-1}(m)\right)/K\right] \qquad (30)$$

In a specific application, V_o, T_{off} and maximum input current I are given, therefore, the design objective is to minimize the normalized energy loss.

$$E_n = \Delta E / \left(2V_o I T_{off}\right) = \frac{(1+m) + \left(\sqrt{1-m^2} - m\cos^{-1}(m)\right)/K}{m\cos^{-1} m} \qquad (31)$$

Eqn (31) is plotted in Fig. 4(a) as a function of m for different valuves of K. in a practicla converter, K is usually within the range of 2-4. A good design should select L_x and C_x so that E_n around its minimum for maximum main inductor current. It can be seen from Fig 4(a) that a good design should have m in the range of [0.5, 0.7].

3.3 The Choice of L_x and C_x

Once m = M is chosen for minimum energy loss and maximum main inductor current. L_x can be calculated as

$$L_x = \frac{V_o T_{off} M}{2I\cos^{-1}(M)}, \qquad C_x = \frac{T_{off} I}{2V_o M\cos^{-1}(M)} \qquad (32)$$

3.4 The Filter Design

The filter design include the design of the input inductor L and the capacitor C_o. The filter inductance, and capacitance can be calculated using the following equations [5].

$$L_o = \frac{V_i(V_o - V_i)}{\Delta I f_s V_o}, \qquad C_o = \frac{I(V_o - V_i)}{V_o f_s \Delta V_{oo}} \qquad (33)$$

Where ΔI and ΔV_{oo} are the change in the output current and the output voltage during one switching cycle.

3.5 The Optimum Inductor Current

E_n for different inductor current i can be written a function of normalized inductor current $I_n = i/I$ as

$$E_n = \frac{\left[(1+MI_n)+\left(\sqrt{1-(MI_n)^2}-MI_n\cos^{-1}(MI_n)\right)\right]K}{M\cos^{-1}(M)} \quad (34)$$

Equation (34) is plotted in Fig. 4(b) for K = 2 and several possible values of M. From Fig 4, it can also be seen that, although an optimum design (here M = 0.6) might have the lowest energy loss in the whole current range, E_n is not very sensitive to M, so M also can be chosen in a relatively large range around its optimum value without significantly reducing the circuit efficiency. Fig 4 can be used to evaluate the circuit efficiency at different currents and to determine whether ZCT is advantageous in efficiency compared to hard switching.

The ZCT schemes can be used to reduce the worst case power dissipation (i.e., at the maximum load) in the power devices. It should be noted that I_{pk} is almost constant, event if the input current is reduced at light load. From Fig. 4(b), we can see that the additional conduction energy loss caused by the soft switching does not change much, even if the main current is reduced from its maximum to zero. Therefore, the ZCT operation should be disabled at light load to achieve god efficiency. Fortunately, the thermal and electrical stresses of device are lower at light load, and the soft-switching function in not relay required.

3.6 The choice of Control Pulse Duration

The conduction duration of the auxiliary switch is always 50% of the resonant cycle, i.e. $T_r/2$. The main switch can be turned on or off around the second resonant peak of i_x, so the delay between the auxiliary switch turn-on signal and the main switch turn-on or turn-off signals can be set to about $3T_r/4$. Therefore, the control timing of the soft-switching is completely independent of the circuit operating point, which greatly simplifies the control design.

4. Experimental Verification

4.1 Experimental Circuit Design

The ZCT PWM boost converter was designed with the following specifications. Input voltage = 50 V, output voltage = 100 V, input current = 2 A, M = 0.7, the switching frequency = 10 kHz, T_{on} = 4 μsec, and the duty cycle = 0.5

4.1.A The Resonant Circuit Design

The resonant components can be calculated using eqn (32) as follows:

$$L_x = \frac{V_o T_r M}{2I\cos^{-1}(M)} = 90\,\mu H$$

$$C_x = \frac{T_r I}{2\cos^{-1}(M)\,M\,V_o} = 72\,nf$$

The characteristic impedance can be calculated as

$$Z_n = \sqrt{L_x/C_x} = 35.3\ ohm$$

And the duration of the resonant period can be calculated as

$$T_r = 2\pi/w_r = 16\,\mu sec$$

Using eqn. (27) the peak current through the auxiliary circuit is

$$I_{pk} = V_o/Z_n = 2.83\ A$$

4.1.B The Drive Circuit

According to the designed values of the auxiliary circuit inductance and capacitance, the synchronized pulses in Fig. 5 are required to control the operation of the designed ZCT converter.

4.1.C The Power Circuit

A 100 w ZCT PWM boost converter with a switching frequency of 10 kHz is built to verify the characteristics of the ZCT technique. The circuit configuration and component values are shown in Fig. 6.

4.2 Experimental Results

Fig. 7 shows the experimentally waveforms for the designed converter. It can be seen that these waveforms are consistent with the theoretically expected waveforms shown in Fig. 2.

Fig. 8 shows a comparison of theoretical and experimentally obtained DC conversion ration of the designed converter theoretically the output voltage is independent on the load, but practically the output voltage in decreases with the increasing of the load current.

The measured efficiency comparison of the ZCT PWM boost converter and the conventional PWM converter is shown in Fig. 9. In this figure, it can be shown that the measured efficiency of the conventional PWM converter is higher than that of the ZCS-PWM converter at light load, but at heavy load the measured efficiency of the ZCS-PWM converter is higher than that of the conventional PWM converter.

Conclusion

The ZCT PWM boost converter has been analyzed, designed and implemented experimentally to obtain moderate power converter by using the power MOSFET as a switch in the main and the auxiliary circuit.

The implemented converter contains the following features:

1. With the help of the auxiliary ZCT circuit, the main switch is turned off under the zero-current condition, practically eliminating all turn-off losses. The turn-on current of the main switch is also reduced to around zero, so switch turn-on loss and diode reverse recovery are also significantly reduced.
2. The auxiliary switches are tuned on and off with zero current.
3. The switches in the ZCT converter have much lower switching loss and switching stress that in a conventional converter and, therefore, can operate at a much higher switching frequency and achieve a much higher power density due to smaller reactive components.
4. The implementation of the ZCT converter is simpler than with a conventional topology, and its cost may be reduced while its efficiency, EMI emission, reliability and dynamic performance are improved.
5. This technique can be used for high power applications by using IGBT as a switch.

References

[1] Carlos, A. Canesin, and Ivo Barbi, "Novel zero-current-switching PWM converters", IEEE Trans. Ind. Electron, Vol. 44, No.3, pp. 372-381, June 1997.

[2] Fred, C. Lee, "High-frequency Quasi-resonant converter technologies", Proceedings of the IEEE, Vol. 76, No. 4, pp. 377-389, April 1988.

[3] Henchun Mao, Fred C. Y. Lee, Xunwei Zhou, Heping Dai, Mohammet Cosan, and Dushan Boroyevich, "Improved zero-current transition converters for high-power applications", IEEE Trans. Ind.

Appl., Vol. 33, No. 5, pp. 1220-1231, September/October 1997.

[4] Jung-Goo Cho, Chang-Yong Jeong, and Fred C. Y. Lee, "Zero-voltage and zero-current-switching full-bridge PWM converter using secondary active clamp", IEEE Trans. Power Electron., Vol. 13, No. 4, pp. 601-607, July 1998.

[5] Muhammed H. Rashid, "Power electronics circuits, devices and applications", Prantice-Hall International, Inc. 1988.

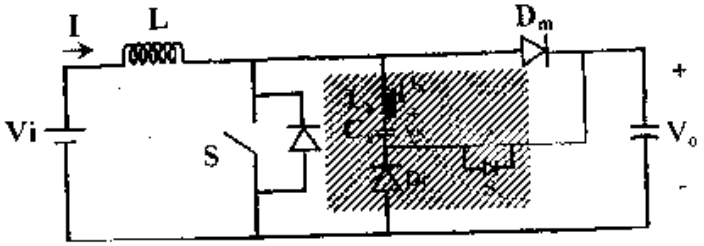

Fig.1 An improved ZCT PWM Converter topology.

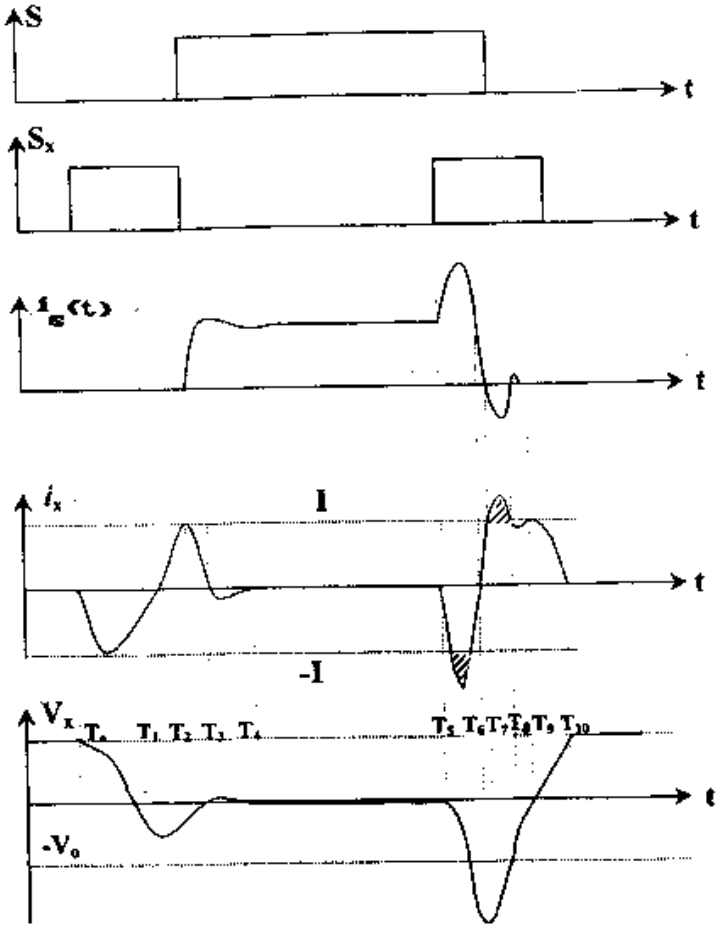

Fig.2 Operating waveforms of the ZCT PWM Converter.

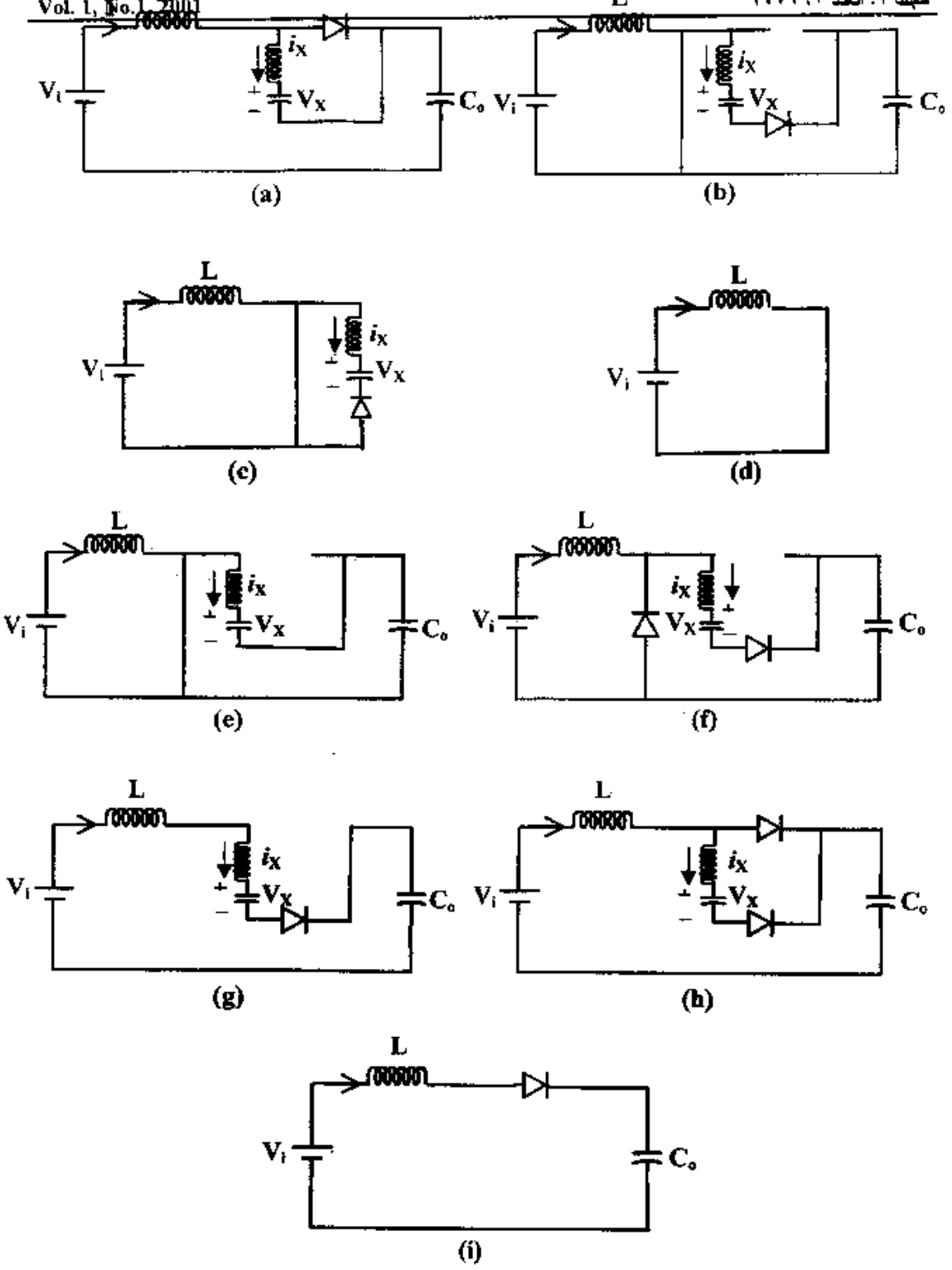

Fig. 3 Operating stages in the soft-switching commutation.

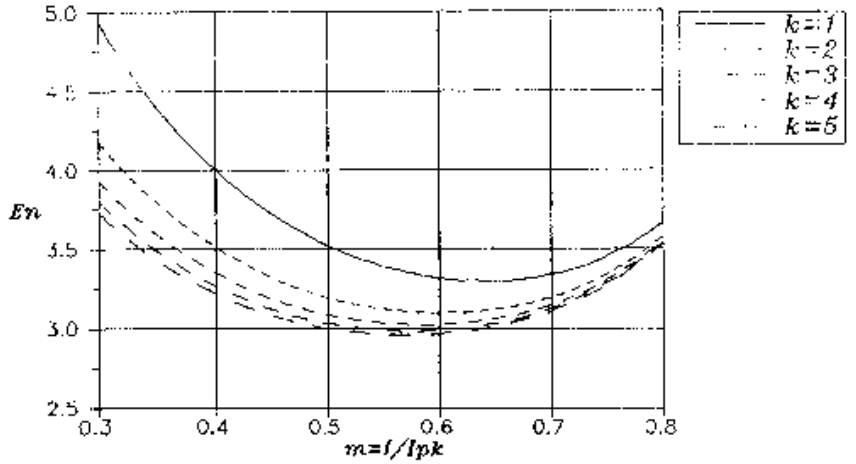

(a)

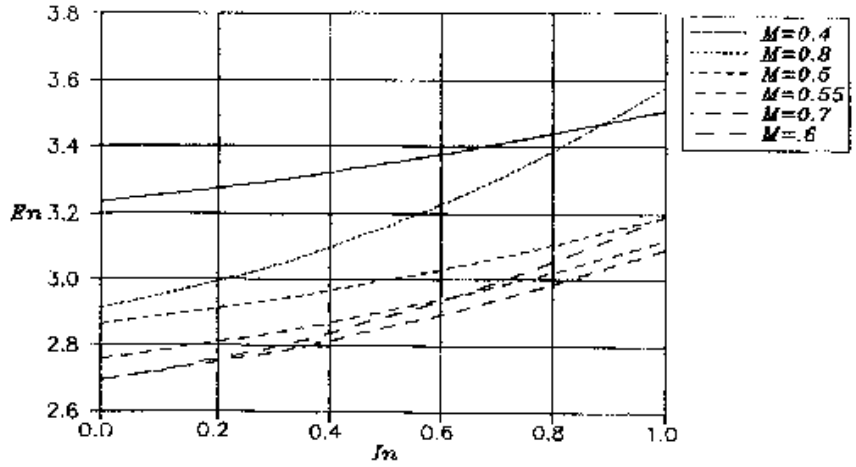

(b)

Fig. 4 Design curves for commutation circuit (a) Additional conduction loss as a function of m (b) Additional conduction loss under different inductor currents.

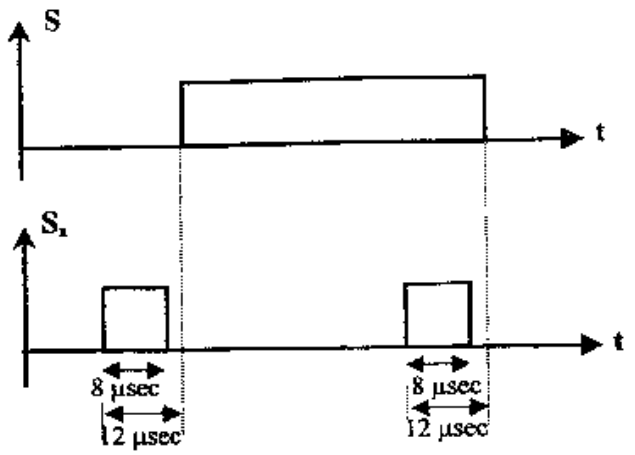

Fig. 5 The required control pulses for the ZCT PWM boost converter.

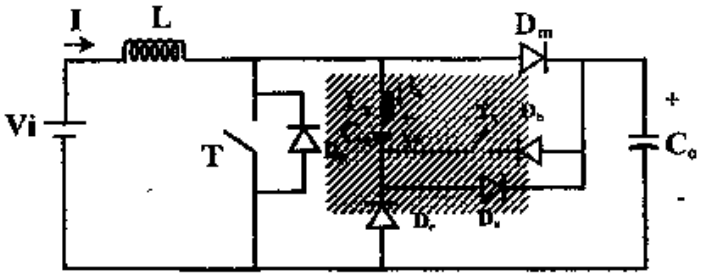

T= VN 4000A Power MOSFET., T_x= VN 4000A Power MOSFET
D_p= D_x=D_b=BYX71., D_c= D= BYW19, L_x=95µH (Ferrite core)
L=6mH, C_x=75nF (Ceramic Capacitance), C_o=1µF

Fig. 6 Practical circuit with components specifications.

i_s
(0.9 A/div , 20 μsec/div)

(a)

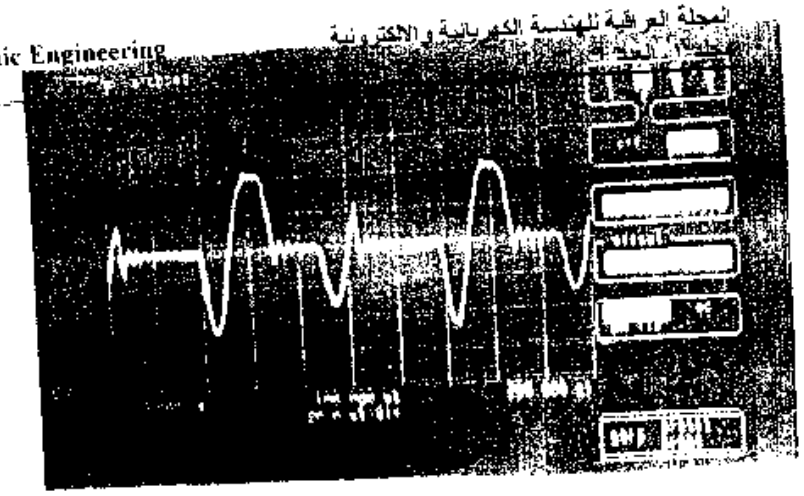

V_s
(100 V/div , 20 μsec/div)

(b)

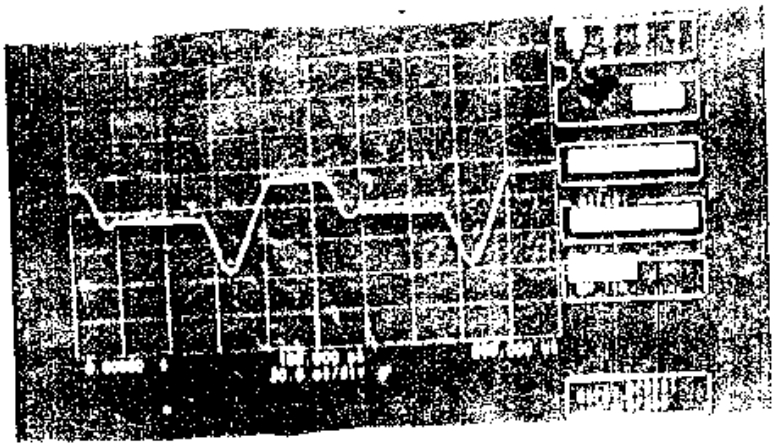

V_{ds} of S
(100 V/div , 20 μsec/div)

i_{ds} of S
(0.9 A/div , 20 μsec/div)

(c)

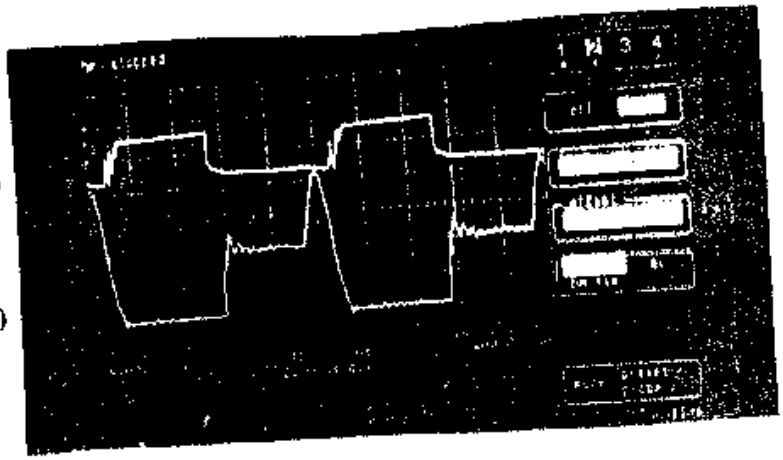

Fig 7 Measured waveforms of the designed converter.

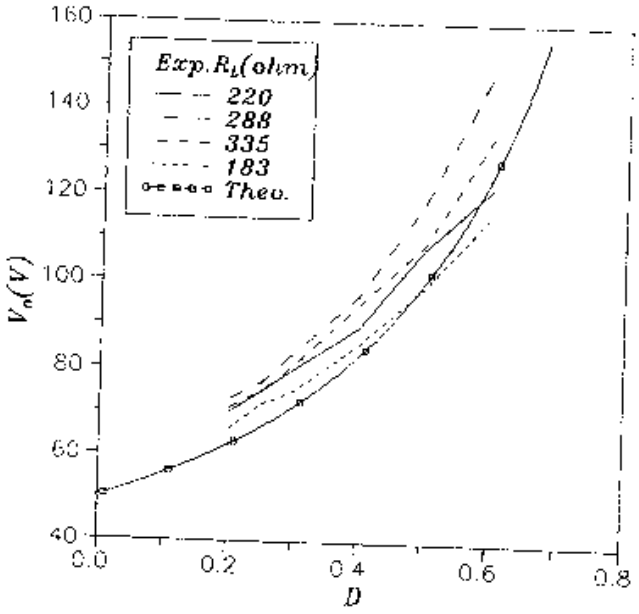

Fig. 8 The change of the output voltage with the duty cycle for the designed converter.

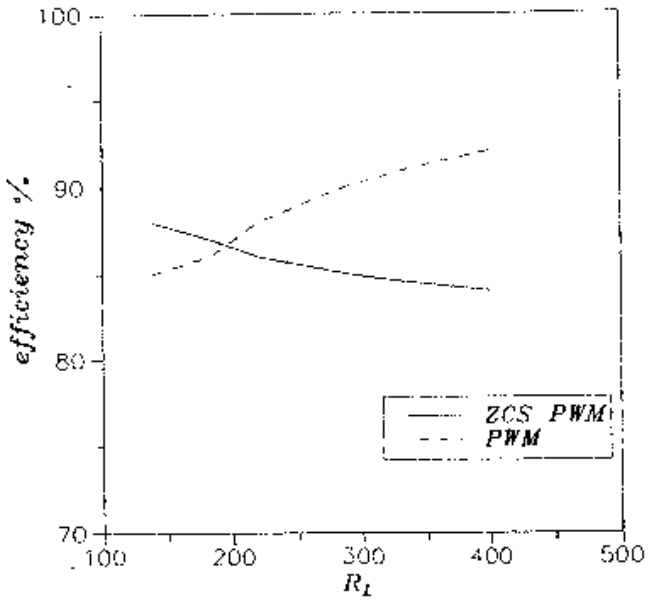

Fig. 9 The change of the measured efficiency with the load for the ZCT PWM converter and conventional PWM converter.